Global NEST Journal, **28** (8), 08452
Available online: 19/10/2026

Human health Risk Assessment and Integrated Contamination Analysis of Potentially Toxic Elements in Urban Soils of Annaba City, Northeast Algeria

Omar Tebboub[1,2], Seifeddine Sellami[3]*, Fares Zaamouche[4,5], Said Lifa[4], Ali Hadjela[6], Ahmed Abderrahim Yahiaoui[7], Redouane Lemoui[2,8], Lotfi Benmekhbi[3] and Ouahida Zeghouan[9]

[1]Department of SM, Faculty of SESNV, Echahid Cheikh Larbi Tebessi University, 12002 Tebessa, Algeria
[2]Research Unit, Valorisation of Natural Resources, Bioactive Molecules and Physicochemical and Biological Analysis (VARENBIOMOL), University of Mentouri Brothers Constantine 1, 25000 Constantine, Algeria
[3]Department of Process Engineering, Faculty of Process Engineering, University of Constantine 3– Salah Boubnider, 25016 Constantine, Algeria
[4]Mines Institute, Echahid Cheikh Larbi Tebessi University, 12002 Tebessa, Algeria
[5]Laboratory of Signals and Smart Systems, Echahid Cheikh Larbi Tebessi University, 12002 Tebessa, Algeria
[6]Department of Earth and Universe Sciences, Faculty of Exact and Life Sciences, Echahid Cheikh Larbi Tebessi University, 12002 Tebessa, Algeria
[7]Laboratory of Physical Chemistry and Biology of Materials, Higher Normal School of Technological Education, ENSET-Skikda, Azzaba, 21000, Algeria
[8]École normale supérieure El Katiba Assia Djebar, Constantine, Algeria
[9]Division Bioindustry, Biotechnology Research Center, 25000 Constantine, Algeria

*Correspondence e-mail: seifeddine.sellami@univ-constantine3.dz

Abstract

Urban soils represent significant sinks for heavy metals and may constitute potential risks to human health, particularly within rapidly urbanizing and industrialized settings. This study assesses the concentrations, spatial distribution, and associated human health risks of cadmium (Cd), copper (Cu), and chromium (Cr) in surface soils of Annaba City, northeastern Algeria. A total of 25 surface-soil samples were collected from systematically selected sampling locations representing the major urban land-use types, including industrial areas, high-traffic corridors, residential neighborhoods, and urban green spaces. One surface-soil sample was collected from each sampling location to characterize the spatial distributionof potentiallytoxic elements at the city scale. The measured concentrations ranged from 0.12 to 14.01 mg kg-1 for Cd, 30.56 to 152.17 mg kg-1 for Cu, and 15.24 to 121.24 mg kg-1 for Cr, with mean concentrations of 1.74, 69.45, and 57.97 mg kg-1, respectively. Among the analyzed metals, cadmium exhibited the greatest spatial variability and the highest degree of enrichment relative to local background levels, with several sampling sites exceeding the regulatory limit of 2 mg kg-1. Pollution assessment using the contamination factor (CF) and geo-accumulation index (Igeo) yielded mean CF values of 17.94, 3.06, and 0.94 and mean Igeo values of 2.05, 0.85, and −0.79 for Cd, Cu, and Cr, respectively. Cadmium exhibited considerable to very high contamination (CF = 1.23–144.43; Igeo = −0.28–6.59), particularly at industrial sites. Copper generally showed moderate contamination, with only a limited number of sampling locations exceeding the regulatory limit of 100 $mg \cdot kg^{-1}$, whereas chromium concentrations remained predominantly within low to moderate contamination classes and did not exceed the regulatory limit (150 mg kg-1) at any sampling location. Geographic information system (GIS)-based spatial analysis identified distinct contamination hotspots, particularly at sites P-14, P-19, and P-24, which spatially correspond to areas influenced by industrial activities. Human health risk assessment (HHRA) indicated that non-carcinogenic hazard index (HI) values were systematically higher for children than for adults. Nevertheless, all estimated HI values remained below the acceptable risk threshold (HI < 1). Cadmium contributed most substantially to the total non-carcinogenic risk at hotspot locations. The estimated carcinogenic risk associated with Cd inhalation was negligible across all sampling sites, remaining several orders of magnitude below the commonly accepted benchmark level (10-6). Multivariate statistical analyses, including principal component analysis and hierarchical cluster analysis, corroborated the observed spatial patterns and emphasized the dominant role of cadmium in controlling contamination variability and differentiating industrially impacted soils from less affected areas. Overall, the integrated application of pollution indices, GIS-based spatial mapping, HHRA, and multivariate techniques identifies cadmium as the principal environmental concern in Annaba's urban soils and provides a robust scientific basis for targeted monitoring strategies and risk-oriented urban soil management.

Keywords: Cadmium; Urban soils; Human health risk assessment; Carcinogenic risk; GIS spatial analysis.

OPEN ACCESS

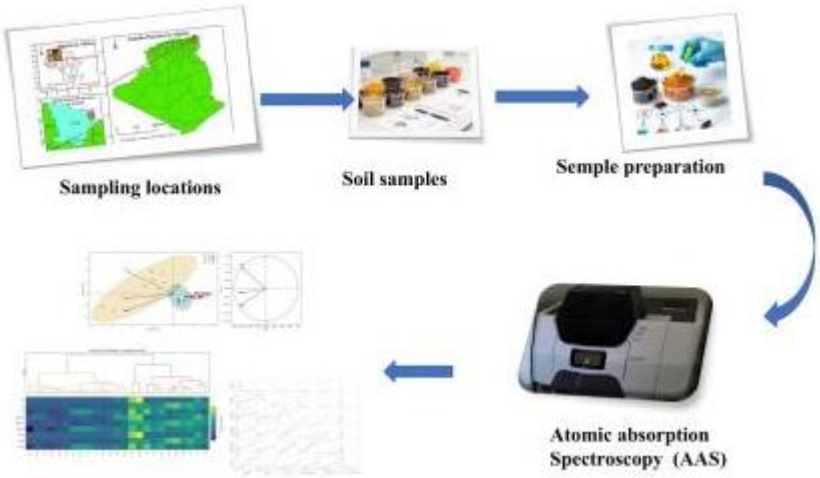
Received: 21/02/2025,

Accepted: 29/09/2025,

Available online: 19/10/2026

Copyright: © 2026 The Author(s). Published in Global NEST Journal. This article is licensed under the terms and conditions of the Creative Commons Attribution 4.0 International license (CC BY 4.0).

Graphical abstract



1. Introduction

Urban soils constitute a fundamental component of urban ecosystems, acting not only as physical supports for infrastructure and vegetation but also as dynamic geochemical interfaces that regulate the accumulation, transformation, and mobility of potentially toxic elements (Gautam *et al.*, 2023; Zwolak *et al.*, 2019). In densely populated urban environments, soils function as long-term sinks for contaminants released by anthropogenic activities such as industrial production, vehicular emissions, port operations, and uncontrolled waste disposal. Unlike agricultural soils, urban soils are subjected to continuous pollutant inputs and frequent human exposure, which enhances their relevance in environmental geochemistry and public health research (Guo *et al.*, 2016; Zhou *et al.*, 2022; Guo *et al.*, 2021). Consequently, the assessment of heavy metal contamination in urban soils has become a central focus of environmental studies worldwide (Abraham *et al.*, 2018; Uwizeyimana *et al.*, 2017).

Heavy metals such as cadmium (Cd), copper (Cu), and chromium (Cr) are of particular concern due to their persistence, non-biodegradability, and contrasting geochemical behaviors in soil systems (Men *et al.*, 2020; Wei *et al.*, 2020; Mameri *et al.*, 2024). Cadmium is a highly toxic and potentially carcinogenic element, commonly associated with industrial emissions, fuel combustion, and urban waste, and even low concentrations may induce adverse health effects (Jiang *et al.*, 2021). Copper, although essential for biological processes, can become toxic at elevated levels and is frequently used as an indicator of traffic-related and industrial pollution (Raimi *et al.*, 2022; Miletić *et al.*, 2023; Liang *et al.*, 2023). Chromium occurs naturally in soils through parent material weathering, but may also be introduced by anthropogenic activities, allowing differentiation between lithogenic and human-induced sources (Pan *et al.*, 2024; Qiao *et al.*, 2023). The combined investigation of Cd, Cu, and Cr therefore provides a comprehensive framework for evaluating contamination intensity, source contributions, and environmental behavior in urban soils (Chen *et al.*, 2023; Zhou *et al.*, 2022; Alhadi & Munaf, 2024).

Annaba City, located in northeastern Algeria, represents a relevant case study due to its rapid urban expansion, high population density, and concentration of heavy industrial activities, including metallurgical complexes, port facilities, and dense transportation networks (Salhi & Dönmez, 2021; Hafiane Hedahdia & Boukhemis, 2024). The coexistence of industrial, residential, and commercial land uses, together with coastal and climatic influences, is expected to enhance spatial heterogeneity in soil contamination patterns (Maas *et al.*, 2010; Qi *et al.*, 2020). Annaba is characterized by a high population density (over 600,000 inhabitants) and hosts extensive industrial infrastructure, including metallurgical complexes, port facilities, and dense transportation networks. These anthropogenic activities make the city particularly susceptible to heavy metal accumulation in urban soils, highlighting the need for a comprehensive assessment of soil contamination and associated human health risks. At a global scale, this local context mirrors the broader challenge of decoupling economic growth from environmental degradation. Recent studies (e.g., Ma *et al.*, 2025) emphasize that sustainable development strategies are crucial for rapidly urbanizing cities like Annaba, enabling continued industrial expansion while minimizing environmental pollution. Despite the city's high vulnerability to such intense environmental pressures,, integrated studies addressing both contamination levels and associated health risks in urban soils of Annaba remain limited (Istanbullu *et al.*, 2023; Seifi *et al.*, 2019). Previous investigations in the region have largely focused on metal concentrations or individual pollution indices, providing limited insight into spatial variability, contamination hotspots, and potential human health implications (Hadif *et al.*, 2020; Saadat, 2022; Umwanzisiwemuremyi *et al.*, 2024). However, existing studies in Annaba have not sufficiently applied high-resolution spatial analysis nor systematically compared

contamination patterns across different land-use types such as industrial, residential, and commercial zones.

Recent studies have demonstrated that urban soils are important sinks for potentially toxic elements and that industrial activities, traffic emissions, and urbanization are the major sources of contamination (Benselhoub *et al.*, 2015; Lifa *et al.*, 2025). These studies have successfully applied pollution indices, GIS-based spatial analysis, and human health risk assessment to evaluate contamination levels and associated health risks, with children generally identified as the most vulnerable population (Aksouh *et al.* 2024). However, such integrated investigations remain limited in northeastern Algeria, particularly in Annaba City, where comprehensive assessments combining contamination indices, spatial analysis, multivariate statistical techniques, and human health risk assessment are still lacking. Therefore, the present study integrates contamination assessment, GIS-based mapping, principal component analysis, hierarchical cluster analysis, and human health risk assessment to characterize the spatial distribution, potential sources, and health risks of Cd, Cu, and Cr in the urban soils of Annaba City.

From a methodological perspective, contamination assessment in urban soils has traditionally relied on indices such as the contamination factor (CF) and the geo-accumulation index (Igeo), which are effective tools for evaluating metal enrichment relative to background levels (Khalili *et al.*, 2021; Nasir *et al.*, 2023; Lu & Bai, 2010; Ksiezopolska, 2002; USDA, 1998). However, these indices do not fully capture the spatial complexity of urban environments, nor do they quantify potential human exposure and associated health risks (Goncharov *et al.*, 2024; Ayaz *et al.*, 2023). Moreover, the combined application of geographic information systems (GIS), human health risk assessment (HHRA), and multivariate statistical techniques remains relatively underdeveloped, particularly in urban soil studies conducted in North African and Mediterranean cities (Ejaz *et al.*, 2025; Gujre *et al.*, 2021). This methodological limitation constrains comprehensive interpretation of contamination processes and the formulation of risk-based soil management strategies (Sun *et al.*, 2021; Peña-Fernández *et al.*, 2014; Qing *et al.*, 2015; Tong *et al.*, 2020).

To address these gaps, the present study adopts an integrated analytical framework combining geochemical pollution indices, GIS-based spatial analysis, human health risk assessment, and multivariate statistical approaches (Ejaz *et al.*, 2025; Sun *et al.*, 2021). The specific objectives are to: (i) quantify the concentrations of Cd, Cu, and Cr in surface soils of Annaba City; (ii) evaluate contamination levels using the contamination factor (CF) and geo-accumulation index (Igeo); (iii) analyze spatial distribution patterns and identify contamination hotspots using GIS techniques; (iv) assess non-carcinogenic and carcinogenic health risks for both children and adults through HHRA; and (v) investigate contamination patterns and potential sources using principal component analysis (PCA) and hierarchical cluster analysis (HCA). By integrating geochemical, spatial, and health-based analyses, this study aims to enhance understanding of urban soil contamination processes and to provide a robust scientific basis for environmental risk assessment and urban soil management in rapidly urbanizing regions.

2. Materials and Methods

2.1. *Study Area*

Annaba Province is located in northeastern Algeria, along the southern margin of the Algerian–Provençal Basin, between latitudes 36°30′–37°30′ N and longitudes 7°20′–8°40′ E (**Figure 1**). **Figure 1** illustrates the location of the study area within Annaba Province rather than depicting the full provincial extent; therefore, the map is intended to provide the geographic context of the investigated urban area rather than the administrative boundaries corresponding to the coordinate range reported above.

The regional climate is Mediterranean, with a mean annual temperature of approximately 18 °C and annual precipitation ranging between 650 and 1,000 mm, predominantly concentrated during the winter season. These climatic conditions, combined with intensive urban and industrial activities, promote the accumulation and redistribution of atmospheric particulates and associated contaminants in surface soils (U.S. EPA, 2007).

From a geological and pedological standpoint, the Annaba region is dominated by sedimentary formations, including limestone, marl, and Quaternary alluvial deposits. Urban soils are generally calcareous and carbonate-rich, which contributes to alkaline pH conditions and strongly influences the retention, mobility, and speciation of heavy metals (Aubert, 1978). These alkaline conditions, derived from the carbonate-rich nature of the soils, play a critical role in controlling the geochemical behavior of heavy metals by enhancing their precipitation, adsorption onto soil particles, and overall retention in the soil matrix.

These properties are particularly relevant for interpreting the behavior of chromium, which is partly controlled by lithogenic inputs, as well as cadmium and copper, which are more responsive to anthropogenic enrichment (Ahmad *et al.*, 2021).

2.2. *Sampling Design and Site Description*

A total of 25 surface soil sampling sites were selected across the urban area of Annaba City (**Table 1; Figure 1**). The sampling design followed a land-use-oriented strategy, combined with a regular spatial distribution, to ensure representative coverage of the main urban functional zones. Sampling locations included industrial areas, high-traffic corridors, residential districts, gardens, cemeteries, and public parks, thereby enabling the identification of spatial variability and potential contamination sources (Diang *et al.*, 2021; AFNOR, 1992).

Sampling sites were approximately distributed on a regular 1 × 1 km grid covering the urban area, with site-specific adjustments implemented to ensure adequate representation of land-use types and accessibility constraints. A systematic spatial configuration was adopted to balance sampling resolution with representative coverage. This approach allows the

characterization of spatial variability and supports the identification of potential contamination sources associated with different anthropogenic activities. Geographic coordinates of all sampling sites were recorded using a handheld GPS receiver and are reported in decimal degrees within the WGS84 coordinate system (**Table S1**). Soil pH determination and background reference considerations followed standardized procedures (AFNOR, 2005; China General Environmental Monitoring Station, 1990). This spatial configuration provides a suitable compromise between spatial resolution and practical feasibility for urban-scale soil contamination assessment.

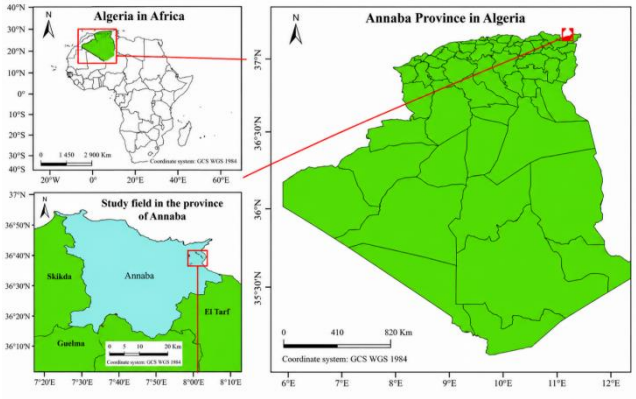


Figure 1. Geographic location of the study area soil samples in Annaba City (top map).

2.3. *Soil Sampling*

Surface soil samples were collected from the uppermost layer of the soil profile (0–5 cm), which is widely regarded as the most relevant horizon for assessing urban contamination due to its direct exposure to atmospheric deposition, industrial dust, and traffic-related emissions. This layer is typically enriched in fine particles, which preferentially accumulate potentially toxic elements, and represents the primary medium for human–soil interaction in urban environments (Chinese Environmental Protection Administration, 1995).

A total of 25 surface-soil samples were collected throughout Annaba City between March and April 2024. Sampling locations were selected using a systematic spatial sampling strategy to provide representative coverage of the principal urban land-use categories across the study area, including industrial areas, high-traffic zones, residential districts, gardens, cemeteries, and public parks (**Table S1; Figure 2**). One surface-soil sample (0–5 cm) was collected from each sampling location. This strategy was designed to characterize the spatial distribution of potentially toxic elements at the city scale rather than to assess micro-scale variability within individual sites. The spatial distribution of the selected sampling locations ensured representative coverage of the study area and facilitated the identification of potential contamination sources associated with different anthropogenic activities.

Sampling sites were approximately distributed on a regular 1 × 1 km grid covering the urban area, with site-specific adjustments implemented to ensure adequate representation of land-use types and accessibility constraints. At each location, approximately 1 kg of surface soil was collected using a stainless-steel spoon previously acid-washed and rinsed with deionized water, thereby minimizing the risk of metal contamination. Samples were immediately placed in clean polyethylene bags and transported to the laboratory (Müller, 1969).

In the laboratory, soil samples were air-dried at room temperature, gently disaggregated, and homogenized using an agate mortar and pestle. The dried material was then sieved through a 2 mm polyethylene mesh to remove coarse fragments and stones. All sampling and preparation equipment was soaked overnight in dilute nitric acid and thoroughly rinsed with deionized water prior to use. Sample handling was conducted using non-metallic tools and protective gloves to prevent cross-contamination. The prepared samples were stored in sealed polyethylene bags until subsequent chemical analysis (Radi *et al.*, 2023).

Each sampling location was represented by a single surface-soil sample (0–5 cm depth) rather than a composite sample prepared from multiple subsamples; consequently, no subsamples were collected within a predefined sampling area at each site. Field duplicate samples and field blanks were not collected as part of the field sampling campaign. Analytical quality assurance and quality control were instead ensured at the laboratory level through reagent blanks, duplicate analyses, certified reference materials (CRM), calibration verification, and recovery assessment.

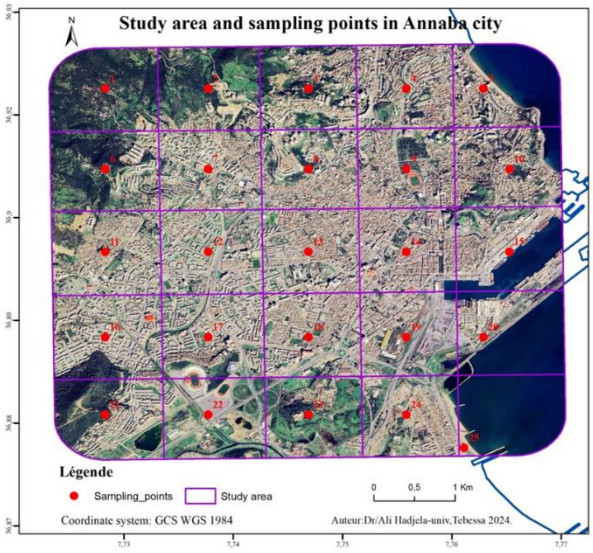


Figure 2. Sampling points and geographic coordinates in decimal degrees of 25 soil samples from the Annaba City region.

2.4. *Determination of Soil pH*

Soil pH was determined using a standard potentiometric method in a soil–water suspension. Briefly, 20 g of air-dried soil was mixed with 50 mL of distilled water, corresponding to a soil-to-water ratio of 1:2.5. The suspension was intermittently stirred and allowed to equilibrate for two hours at room temperature prior to measurement. Soil pH was measured using a calibrated digital pH meter (Inolab pH 7310, Germany) (Golia *et al.*, 2019).

The pH meter was calibrated at the beginning of each analytical series using standard buffer solutions at pH 4.0, 7.0, and 10.0 to ensure measurement accuracy and

reproducibility. This method is widely applied for characterizing soil acidity–alkalinity conditions and provides reliable information for interpreting heavy metal mobility and retention in soils (Arab *et al.*, 2021).

2.5. *Sample Preparation and Chemical Analysis*

Heavy metal concentrations in soil samples were determined using aqua regia extraction, followed by atomic absorption spectroscopy (AAS). The digestion procedure was conducted in accordance with ISO 11466 (1995), which yields pseudo-total metal concentrations suitable for environmental contamination assessment. Approximately 5 g of homogenized soil was placed in a Pyrex digestion vessel, and a mixture of concentrated hydrochloric acid (HCl, 37%) and nitric acid (HNO_3, 70%), in a volumetric ratio of 3:1, was added (Zhanibekov *et al.*, 2022).

The samples were heated on a hot plate at approximately 130 °C for 30 minutes until near dryness, in order to enhance the dissolution of metal-bearing phases. After cooling, the residue was re-dissolved in 1.6 M nitric acid, centrifuged to remove insoluble particles, and the supernatant was filtered through Whatman N° 42 filter paper. The filtrate was quantitatively transferred into a 25 mL volumetric flask and diluted to volume with distilled water (Chileshe *et al.*, 2020).

Concentrations of cadmium (Cd), copper (Cu), and chromium (Cr) were measured using flame atomic absorption spectroscopy with an air–acetylene flame (Shimadzu AA-7000, Japan) (Bołzan, 2017). Instrument calibration was carried out using multi-element standard solutions prepared in the same acid matrix as the samples. To ensure the accuracy and reliability of the analytical procedures, a Certified Reference Material for soil analysis was digested and analyzed alongside the field samples. The recovery rates obtained were 97% for Cd, 101% for Cu, and 98% for Cr. Analytical quality control procedures routinely included the analysis of procedural blanks and duplicate samples to ensure analytical precision and to minimize potential contamination. The relative standard deviation (RSD) for all replicate analyses remained consistently below 5%, demonstrating high analytical precision.The applied methodology provides highly reliable and reproducible concentration data for assessing heavy metal contamination in urban soils (Chen *et al.*, 2021).

2.6. *Assessment of Soil Contamination by Heavy Metals*

Soil contamination by heavy metals was assessed using widely applied geochemical pollution indices that compare measured metal concentrations with reference background levels. In this study, the contamination factor (CF) and the geo-accumulation index (Igeo) were employed to evaluate the degree of metal enrichment and pollution of cadmium (Cd), copper (Cu), and chromium (Cr) in urban surface soils (Wang *et al.*, 2022; Xiao *et al.*, 2024; Bartoszek *et al.*, 2022).

2.6.1. Contamination Factor (CF)

The contamination factor (CF) was calculated as the ratio between the measured concentration of a given metal in soil (C_n) and its corresponding background concentration (B_n), according to the following equation:

$$CF = \frac{C_n}{B_n}$$

where C_n represents the concentration of metal n in the soil sample ($mg \cdot kg^{-1}$), and B_n denotes the geochemical background concentration of the same metal. (Goher *et al.*, 2019; El Zrelli *et al.*, 2015).

Based on CF values, soil contamination was classified into four categories: CF < 1 (low or no contamination), 1 ≤ CF < 3 (moderate contamination), 3 ≤ CF< 6 (considerable contamination), and CF ≥ 6 (very high contamination) (Islam *et al.*, 2022).

2.6.2. 2.6.2. Geo-accumulation Index (Igeo)

The geo-accumulation index (Igeo), originally proposed by Müller (1969), was used to assess the degree of metal accumulation in soils relative to background concentrations, while accounting for natural geochemical variability. The Igeo was calculated using the following equation:

$$I_{geo} = log_2\left(\frac{C_n}{1.5 \times B_n}\right)$$

where C_n is the measured concentration of the metal in the soil sample, B_n is the corresponding background concentration, and the factor 1.5 accounts for possible natural variations in background values due to lithological differences (Bi *et al.*, 2018; Baran & Wieczorek, 2015).

According to established classification criteria, Igeo ≤ 0 indicates unpolluted conditions; 0 < Igeo ≤ 1 indicates unpolluted to moderately polluted soils; 1 < Igeo ≤ 2 moderately polluted; 2 < Igeo ≤ 3 moderately to strongly polluted; 3 < Igeo ≤ 4 strongly polluted; 4 < Igeo ≤ 5 strongly to extremely polluted; and Igeo > 5 extremely polluted soils (Zahra *et al.*, 2014; Khalili *et al.*, 2021; Nasir *et al.*, 2023).

The combined application of CF and Igeo provides complementary information on metal enrichment and pollution intensity and was subsequently used to support spatial analysis, multivariate statistical interpretation, and human health risk assessment.

The background values (B_n) used in this study were adopted from the Chinese Soil Environmental Quality Standard (GB15618-1995) (CEPA, 1995). These values are widely employed in the calculation of contamination indices, particularly the geoaccumulation index (Igeo), and provide a standardized reference framework that facilitates comparison with numerous international studies. The same reference has also been used in previous studies conducted in Algeria (Sellami *et al.*, 2022), ensuring methodological consistency.

2.7. *Human Health Risk Assessment*

Human health risk assessment (HHRA) was performed to evaluate potential non-carcinogenic and carcinogenic risks associated with exposure to heavy metals in urban soils of Annaba City for both children and adults. The assessment

followed the methodological framework recommended by the United States Environmental Protection Agency (USEPA) and considered the principal exposure pathways relevant to urban environments (Strenge & Chamberlain, 1995).

To ensure full transparency and reproducibility of the exposure assessment, all exposure factors and toxicological reference values used to calculate the average daily dose (ADD), hazard quotient (HQ), hazard index (HI), and carcinogenic risk (CR) for the ingestion and dermal contact pathways, separately for children and adults are compiled in **Table 1**.

Table 1. Exposure parameters and toxicological reference values used in the Human Health Risk Assessment (HHRA)

Parameter	Symbol	Children	Adults	Unit	Reference
Body weight	BW	15	70	kg	USEPA (2011)
Soil ingestion rate	IR_soil	200	100	mg day^{-1}	USEPA (2011)
Inhalation rate	IR_air	7.63	20	m^3 day^{-1}	USEPA (2011)
Exposure frequency	EF	350	350	days year^{-1}	USEPA (2011)
Exposure duration	ED	6	24	years	USEPA (2011)
Averaging time (non-carcinogenic)	AT_nc	2,190	8,760	days	USEPA (2011)
Averaging time (carcinogenic)	AT_c	25,550	25,550	days	USEPA (2011)
Skin surface area	SA	2,800	5,700	cm^2	USEPA (2011)
Soil adherence factor	AF	0.20	0.07	mg cm^{-2}	USEPA (2011)
Dermal absorption factor	ABS	0.001	0.001	–	USEPA (2004)
Particle emission factor	PEF	1.36×10^9	1.36×10^9	m^3 kg^{-1}	USEPA (2002)
Conversion factor	CF	10^{-6}	10^{-6}	kg mg-1	USEPA (1989)
Oral reference dose – Cd	RfD_ing	1×10^{-3}	1×10^{-3}	mg kg^{-1}day^{-1}	USEPA IRIS
Dermal reference dose – Cd	RfD_derm	2.5×10^{-5}	2.5×10^{-5}	mg kg^{-1} day^{-1}	USEPA IRIS
Oral reference dose – Cu	RfD_ing	4×10^{-2}	4×10^{-2}	mg kg^{-1} day^{-1}	USEPA IRIS
Dermal reference dose – Cu	RfD_derm	1.2×10^{-2}	1.2×10^{-2}	mg kg^{-1} day^{-1}	USEPA IRIS
Oral reference dose – Cr	RfD_ing	3×10^{-3}	3×10^{-3}	mg kg^{-1}day^{-1}	USEPA IRIS
Dermal reference dose – Cr	RfD_derm	7.5×10^{-5}	7.5×10^{-5}	mg kg^{-1} day^{-1}	USEPA IRIS
Cancer slope factor (Cd, inhalation)	SF_inh	6.3	6.3	(mg kg^{-1} day^{-1})$^{-1}$	USEPA IRIS

All parameter values applied in this study are consistent with the USEPA (2011) Exposure Factors Handbook and the USEPA Regional Screening Level / Integrated Risk Information System (IRIS) toxicological databases, thereby ensuring compliance with internationally recognized risk assessment guidelines and enabling full reproducibility of the reported HQ, HI, and CR values across all sampling sites.

2.7.1. Exposure Pathways and Average Daily Dose

For non-carcinogenic effects, exposure through accidental soil ingestion and dermal contact was considered, whereas inhalation of resuspended soil particles was evaluated exclusively for carcinogenic risk. Separate exposure scenarios were defined for children and adults to account for differences in physiological characteristics, behavior patterns, and exposure duration (Strenge & Chamberlain, 1995).

Average daily doses (ADDs) were calculated for each metal and sampling site using the following equations:

$$ADD_{ing} = \frac{C \times IR \times EF \times ED}{BW \times AT} \times 10^{-6}$$

$$ADD_{derm} = \frac{C \times SA \times AF \times ABS \times EF \times ED}{BW \times AT} \times 10^{-6}$$

$$ADD_{inh} = \frac{C \times IR_{air} \times EF \times ED}{PEF \times BW \times AT}$$

where C represents the metal concentration in soil (mg·kg^{-1}), and the remaining parameters describe exposure frequency (EF), exposure duration (ED), body weight (BW), averaging time (AT), and pathway-specific exposure factors. The conversion factor (10^{-6}) was applied to convert soil concentrations from mg·kg^{-1} to kg·kg^{-1} (McKone & Daniels, 1991).

2.7.2. Non-Carcinogenic Risk Assessment

Non-carcinogenic risk was evaluated using the hazard quotient (HQ), defined as the ratio between the estimated average daily dose (ADD) and the corresponding reference dose (RfD):

$$HQ = \frac{ADD}{RfD}$$

The hazard index (HI), representing the cumulative non-carcinogenic risk arising from multiple exposure pathways and metals, was calculated as the sum of individual HQ values:

$$HI = \sum HQ$$

An HI value lower than unity (HI < 1) indicates that adverse non-carcinogenic health effects are unlikely under the assessed exposure conditions (Cai *et al.*, 2019).

2.7.3. Carcinogenic Risk Assessment

Carcinogenic risk (CR) was estimated for cadmium (Cd) via inhalation exposure using the cancer slope factor (SF) approach:

$$CR = ADD_{inh} \times SF$$

Cadmium was selected for carcinogenic risk assessment due to its recognized carcinogenicity through inhalation pathways. Chromium was excluded from carcinogenic risk calculations, as the present study quantified total chromium concentrations without chemical speciation, thereby preventing differentiation between trivalent [Cr(III)] and hexavalent [Cr(VI)] forms. According to international risk assessment guidelines, acceptable lifetime cancer risk values generally range from 10^{-6} to 10^{-4}, whereas values below 10^{-6} are considered negligible (Yousefi *et al.*, 2022).

2.8. *Statistical Analysis*

Statistical analyses were conducted to examine relationships among heavy metals, assess spatial variability, and identify potential contamination patterns and sources in urban soils. All statistical analyses were performed on metal concentration data obtained from 25 sampling sites (n = 25) using IBM SPSS Statistics version 26.0 (IBM Corp., Armonk, NY, USA). A significance level of $p < 0.05$ was adopted for all statistical tests. Graphical representations were prepared using OriginPro 2023 (OriginLab Corporation, Northampton, MA, USA), and descriptive calculations were verified using Microsoft Excel 2021 (Microsoft Corporation, Redmond, WA, USA).

Data normality was evaluated using the Shapiro–Wilk test, which is appropriate for small sample sizes. When data followed a normal distribution, differences among sampling sites were assessed using one-way analysis of variance (ANOVA); otherwise, the non-parametric Kruskal–Wallis test was applied. Homogeneity of variances was evaluated prior to the application of ANOVA. Prior to multivariate statistical analyses, metal concentration data were log-transformed to reduce skewness and standardized using z-score transformation to ensure equal weighting of variables (Shukla *et al.*, 2024).

Principal component analysis (PCA) was applied to identify the main factors controlling the distribution of Cd, Cu, and Cr in urban soils. PCA was performed using the correlation matrix, and component retention was based on the Kaiser criterion (eigenvalues > 1), supported by visual inspection of the scree plot. The percentage of total variance explained by each principal component was used to evaluate their relative contribution and importance (Szczepanik *et al.*, 2021).

Hierarchical cluster analysis (HCA) was conducted to classify sampling sites according to similarities in metal concentrations. Clustering was performed using Euclidean distance as a measure of similarity and Ward's linkage method, selected for its effectiveness in minimizing within-cluster variance. The optimal number of clusters was determined based on visual inspection of the dendrogram, in combination with consistency with observed spatial patterns and land-use characteristics. The combined application of PCA and HCA provided complementary insights into contamination patterns and supported the identification of dominant controlling factors and potential sources of heavy metals in urban soils (Thavamani *et al.*, 2012).

2.9. *GIS-Based Spatial Interpolation*

Spatial distribution maps of the measured concentrations of Cd, Cu, and Cr and their corresponding pollution indices, including the geoaccumulation index (Igeo) and contamination factor (CF), were generated from the point-based measurements obtained at the 25 sampling sites using Python 3. The spatial interpolation was performed using the scipy.interpolate.griddata function from the SciPy library, with cubic interpolation (method='cubic'), while Matplotlib was used for graphical visualization and map generation. A regular 200 × 200 cell grid was generated over the sampling domain, covering longitude 7.7309°–7.7650° E and latitude 36.8833°–36.9088° N, with a 0.003° buffer added around the spatial extent of the sampling sites. All interpolation procedures were conducted in geographic coordinates using the WGS 84 datum (EPSG:4326), consistent with the GPS coordinates recorded at the 25 sampling locations.

The measured concentration ranges used for the spatial analysis were 0.12–14.01 mg kg^{-1} for Cd (mean = 1.74 mg kg^{-1}), 30.56–152.17 mg kg^{-1} for Cu (mean = 69.45 mg kg^{-1}), and 15.24–121.24 mg kg^{-1} for Cr (mean = 57.97 mg kg^{-1}). The corresponding Igeo values ranged from 0.5 to 6.4 for Cd, −0.1 to 1.5 for Cu, and −2.3 to 0.5 for Cr, whereas the CF values ranged from 10.5 to 104.0 for Cd, 1.6 to 5.2 for Cu, and 0.3 to 1.9 for Cr.

The reliability of the interpolated surfaces was evaluated using leave-one-out cross-validation (LOOCV) for each mapped variable. In this procedure, each sampling site was sequentially excluded from the dataset, its value was re-estimated using the remaining n − 1 observations and the same cubic interpolation procedure, and the residual was calculated as the difference between the predicted and observed values. The resulting root mean square error (RMSE) values were 2.07 mg kg^{-1} for Cd, 12.7 mg kg^{-1} for Cu, and 51.6 mg kg^{-1} for Cr. For the corresponding Igeo values, the RMSEs were 1.20 for Cd, 0.58 for Cu, and 0.86 for Cr, while the RMSEs for CF were 23.6 for Cd, 1.07 for Cu, and 0.63 for Cr. These validation results are reported in **Table 2** and provide a quantitative assessment of interpolation uncertainty. The comparatively larger RMSE associated with Cr indicates greater interpolation uncertainty for this element, which may reflect stronger spatial heterogeneity in its distribution across the study area. Accordingly, the interpolated maps are interpreted as spatial representations of the observed concentration and index patterns, with consideration given to the associated interpolation uncertainty.

3. Results and Discussion

3.1. *Evolution of Soil pH*

The spatial distribution of soil pH values measured across the 25 sampling sites is presented in Table S2 and illustrated in **Figure 3**. Soil pH values ranged from 7.2 to 7.9, with a mean value of 7.6 and a low standard deviation (±0.16), indicating relatively homogeneous alkaline conditions throughout the study area.

The observed alkaline pH values can be primarily attributed to the carbonate-rich nature of urban soils in the Annaba region, which is consistent with the underlying sedimentary geology dominated by limestone and other calcareous formations (AFNOR, 1992; AFNOR, 2005). The limited spatial variability of soil pH suggests that soil acidity–alkalinity is not a dominant factor controlling the spatial differentiation of metal concentrations within the study area.

From a geochemical standpoint, alkaline soil conditions generally reduce the mobility and bioavailability of many heavy metals by enhancing adsorption onto mineral surfaces and favoring precipitation as carbonates or hydroxides (Bołzan, 2017; Chen *et al.*, 2021). This behavior is particularly relevant for chromium, which tends to exhibit low mobility under alkaline conditions, thereby supporting its predominantly lithogenic control, as indicated by the pollution indices and multivariate statistical analyses (Bi *et al.*, 2018; Baran & Wieczorek, 2015). In contrast, the elevated concentrations and enrichment of cadmium and copper observed at specific sites cannot be satisfactorily explained by pH variability alone and are therefore more plausibly associated with localized anthropogenic inputs (Wang *et al.*, 2022; Xiao *et al.*, 2024).

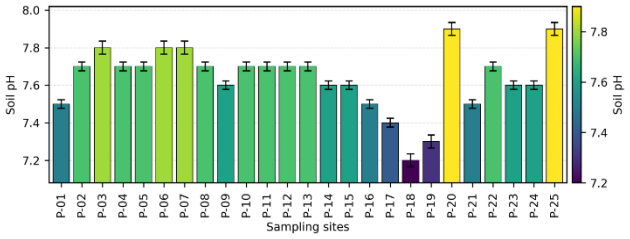


Figure 3. Spatial variation of soil pH across sampling sites in the Annaba City region.

Overall, the alkaline and spatially uniform pH conditions characterizing Annaba's urban soils provide a stable geochemical background, against which the influence of anthropogenic sources on heavy metal accumulation can be more clearly discerned.

Soil pH values ranged from 7.2 to 7.9 (mean = 7.6 ± 0.16), indicating spatially uniform alkaline conditions across the study area. This alkalinity, most likely associated with the carbonate-rich nature of the soils, generally reduces the mobility of heavy metals. The limited spatial variability of pH suggests that the observed differences in metal concentrations are primarily governed by localized anthropogenic inputs, rather than by variations in soil acidity.

3.2. *Heavy Metal Concentrations*

The concentrations of cadmium (Cd), copper (Cu), and chromium (Cr) measured in surface soils of Annaba City are summarized in **Table 3** and illustrated in **Figures 5, 6**. The results exhibited pronounced spatial variability, reflecting heterogeneous anthropogenic influences across the urban area.

Cadmium concentrations ranged from 0.12 to 14.01 mg·kg^{-1}, with a mean value of 1.74 mg·kg^{-1}, substantially exceeding the local background level (0.097 mg·kg^{-1}). Although most sampling sites displayed Cd concentrations below the French regulatory limit of 2 mg·kg^{-1} (AFNOR U44-041), several locations, notably P-14, P-19, and P-24, exceeded this threshold by approximately one order of magnitude. These sites therefore represent localized contamination hotspots, indicating significant anthropogenic Cd enrichment.

Copper concentrations varied between 30.56 and 152.17 mg·kg^{-1}, with an average concentration of 54.99 mg·kg^{-1}, consistently higher than the background value (22.6 mg·kg^{-1}). While the majority of sampling sites remained below the regulatory limit of 100 mg·kg^{-1}, exceedances were recorded at several locations, particularly in areas subject to industrial influence and intense traffic activity. This distribution pattern suggests a spatially extensive but generally moderate level of Cu contamination throughout the study area.

Chromium concentrations ranged from 15.24 to 121.24 mg·kg^{-1}, with a mean value of 53.79 mg·kg^{-1}, which is close to the regional background concentration (61 mg·kg^{-1}) and well below the regulatory limit of 150 mg·kg^{-1}. The relatively limited variability and the absence of regulatory exceedances indicate that Cr contamination is comparatively low and is predominantly controlled by lithogenic inputs, with only minor localized anthropogenic contributions (**Figure 4**).

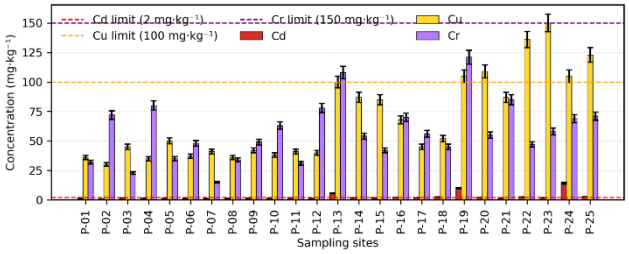


Figure 4. Concentrations of Cd, Cu, and Cr in soil samples collected from the Annaba City region.

Overall, comparative evaluation of the three metals identifies cadmium as the most critical contaminant in Annaba's urban soils, due to its pronounced enrichment relative to background levels and the occurrence of distinct hotspots exceeding regulatory thresholds. Copper exhibits moderate but spatially widespread enrichment, whereas chromium shows the lowest contamination levels and poses limited environmental concern under current conditions.

3.2.1. Spatial Patterns and Source Attribution

Spatial distribution maps (**Figure 5**) reveal that elevated Cd concentrations are predominantly clustered near industrial zones, particularly in the vicinity of the El Hadjar iron and steel complex, suggesting a likely contribution from industrial emissions.

The geogenic interpretation for Cr is further reinforced by its weak correlation with soil pH and by the prevailing alkaline conditions observed across the study area. Under such conditions, chromium is expected to occur predominantly in its stable trivalent form, Cr(III), which exhibits low solubility due to precipitation as chromium

hydroxides and strong adsorption onto clay minerals and Fe–Mn oxide surfaces. Because soil pH values remain consistently within the alkaline range, minor spatial fluctuations are unlikely to significantly affect Cr mobility, bioavailability, or redistribution. Consequently, the weak statistical association between Cr concentrations and soil pH reflects limited geochemical remobilization and supports the persistence of chromium within the parent material. This restricted mobility provides a plausible explanation for the relatively uniform spatial distribution of Cr and is consistent with a predominantly lithogenic origin.

The identification of distinct Cd hotspots around the El Hadjar steel complex highlights the need for strengthened environmental management strategies in highly industrialized sectors of Annaba. While conventional pollution-control measures and regulatory enforcement remain essential, increasing attention should also be directed toward industrial green innovation as a proactive mechanism for reducing contaminant emissions at their source. Recent evidence suggests that environmental regulatory policies can incentivize industrial enterprises to adopt cleaner production technologies and enhance environmental performance through innovation-driven processes (Zhang *et al.*, 2025). Therefore, integrating effective regulatory frameworks with policies that promote green technological innovation could constitute a sustainable approach for mitigating heavy-metal contamination, reducing industrial environmental impacts, and improving long-term soil quality and ecosystem resilience in rapidly urbanizing industrial regions.

Additional diffuse contributions to Cd and Cu may arise from agricultural practices, including phosphate fertilizer application, as well as from traffic-related emissions, such as brake and tire wear. The partial spatial overlap of Cd and Cu enrichment patterns underscores the cumulative influence of multiple anthropogenic sources in shaping urban soil contamination.

Although elevated Cd concentrations were observed near major industrial facilities, the present study did not include direct source-apportionment analyses, industrial emission inventories, prevailing wind data, or distance-to-source analyses. Therefore, the proposed industrial influence should be regarded as a plausible interpretation based on the observed spatial patterns and surrounding land-use characteristics rather than definitive evidence of contamination sources. Future studies integrating receptor models, land-use overlay analysis, atmospheric transport information, and emission inventories would provide stronger support for source identification.

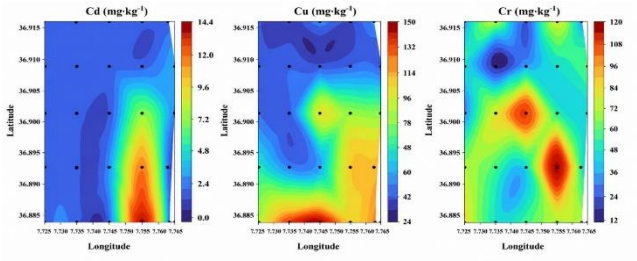


Figure 5. Spatial distribution of Cd, Cu and Cr concentrations in urban soils from the Annaba City region.

3.3. *Assessment of soil contamination using Igeo and CFindices*

To further evaluate the intensity and sources of heavy metal contamination in the urban soils of Annaba City, the geo-accumulation index (Igeo) and the contamination factor (CF) were calculated for cadmium (Cd), copper (Cu), and chromium (Cr) at each sampling site. These indices provide complementary information on metal enrichment relative to natural background levels and allow the assessment of contamination intensity and spatial variability across the study area. The minimum, maximum, and mean values obtained for each element are summarized in **Table 2**.

Table 2. Geo-accumulation index (I*geo*) and contamination factor (CF) values for Cd, Cu, and Cr in soil samples from the Annaba City region.

POSİTİONS	IGEO			CF		
	Cd	**Cu**	**Cr**	**Cd**	**Cu**	**Cr**
P-01	-0,.28	0.12	-1.51	1.23	1.62	0.52
P-02	1.04	-0.15	-0.34	3.09	1.35	1.18
P-03	-0.06	0.42	-1.98	1.44	2.00	0.38
P-04	0.94	0.06	-0.18	2.88	1.55	1.32
P-05	0.04	0.58	-1.38	1.54	2.23	0.57
P-06	0.31	0.14	-0.92	1.85	1.65	0.79
P-07	1.35	0.28	-2.59	3.81	1.82	0.24
P-08	1.66	0.12	-1.39	4.74	1.63	0.57
P-09	1.31	0.30	-0.88	3.71	1.84	0.81
P-10	4.14	0.15	-0.55	26.49	1.66	1.02
P-11	1.56	0.29	-1.54	4.43	1.83	0.51
P-12	1.04	0.24	-0.23	3.09	1.76	1.28
P-13	0.94	1.56	0.25	2.88	4.41	1.78
P-14	5.38	1.37	-0.75	62.68	3.87	0.89
P-15	3.02	1.34	-1.10	12.16	3.79	0.69
P-16	1.31	1.02	-0.39	3.71	3.03	1.14
P-17	-0.06	0.44	-0.70	1.44	2.02	0.92

P-18	3.55	0.62	-0.99	17.62	2.31	0.75
P-19	6.12	1.65	0.41	104.63	4.70	1.98
P-20	3.16	1.69	-0.72	13.40	4.85	0.90
P-21	1.89	1.37	-0.10	5.56	3.87	1.39
P-22	1.42	2.01	-0.95	4.02	6.05	0.77
P-23	2.09	2.17	-0.65	6.39	6.73	0.95
P-24	6.59	1.64	-0.40	144.43	4.67	1.13
P-25	2,93	1,86	-0,37	11,44	5,45	1,15
Min	-0.28	-0.15	-2.59	1.23	1.35	0.24
Max	6.59	2.17	0.41	144.43	6.73	1.98
Mean	2.05	0.85	-0.79	17.94	3.06	0.94

3.3.1. Spatial patterns of Igeo and CF

As shown in **Table 2 and Figure 6**, Igeo values for Cd range from −0.28 to 6.59, indicating conditions ranging from unpolluted to extremely polluted. Several sites exhibit Igeo values greater than 5, classifying them as heavily to extremely contaminated and reflecting strong anthropogenic enrichment. In contrast, Cu shows Igeo values between −0.15 and 2.17, corresponding mainly to uncontaminated to moderately contaminated conditions. Chromium displays the lowest Igeo values (−2.59 to 0.41), suggesting predominantly unpolluted to slightly polluted soils.

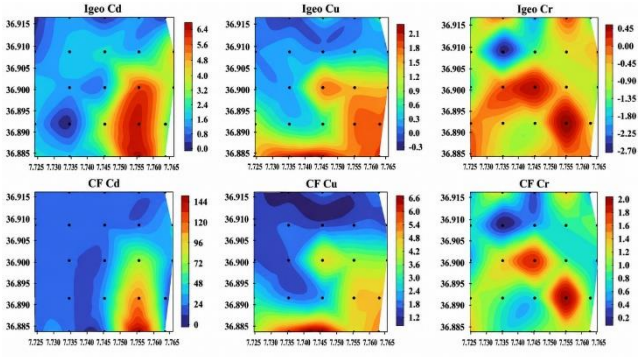


Figure 6. Spatial distribution of geo-accumulation index (I*geo*) and contamination factor (C*F*) for Cd, Cu, and Cr in urban soils from the Annaba City region.

The contamination factor further supports these patterns. CF values for Cd vary widely from 1.23 to 144.43, indicating considerable to very high contamination at several locations. Copper exhibits moderate to high contamination (CF= 1.35–6.73), whereas Cr shows low to moderate contamination levels (CF = 0.24–1.98), with most sites remaining close to natural background conditions.

3.3.2. Igeo–CF consistency and source implications

Measured cadmium (Cd) concentrations were the highest relative to the adopted background values and showed pronounced spatial variability across the study area, with the greatest concentrations recorded at sites P-14, P-19, and P-24. A consistent co-variation between Igeo and CF values was observed and reflected the measured enrichment pattern, providing complementary quantitative measures of contamination severity rather than independent evidence of contamination. These sites correspond to areas influenced by industrial activities, thereby supporting an anthropogenic origin for Cd contamination in conjunction with the measured concentrations and the spatial distribution pattern (**Figure 7**).

Measured Cu concentrations were elevated at several industrial and high-traffic locations. Copper shows corresponding moderate Igeo–CF values that are consistent with these measured concentrations, suggesting mixed anthropogenic and geogenic contributions, likely associated with industrial emissions and traffic-related sources.

Measured Cr concentrations displayed relatively limited spatial variability and generally remained close to the adopted background value. In contrast, chromium exhibits weak enrichment, with CF values close to unity and predominantly negative Igeo values, which are consistent with a mainly lithogenic origin and limited anthropogenic impact under the alkaline soil conditions prevailing in the study area.

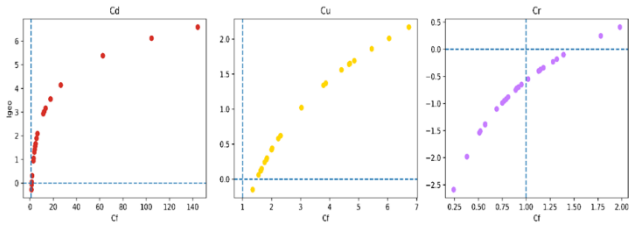


Figure 7. Relationship between the geo-accumulation index (Igeo) and contamination factor (CF) for Cd, Cu, and Cr in soils from the Annaba City region.

Overall, the measured concentrations, their spatial distribution, and their relationship with surrounding land-use characteristics identify cadmium as the principal contaminant of concern in the urban soils of Annaba. The calculated Igeo and CF indices provide quantitative measures of the degree of enrichment relative to background values and facilitate comparison with previous studies. Copper exhibited moderate enrichment, whereas chromium generally reflected background geochemical conditions and a predominantly lithogenic origin. These findings provide a quantitative basis for prioritizing sites for further evaluation and support the subsequent human health risk assessment.

4. Human Health Risk Assessment

The human health risk assessment indicates that non-carcinogenic risks (HI) for both children and adults remain below the acceptable threshold (HI < 1) across all sampling sites, suggesting that adverse health effects are unlikely

under current exposure conditions. **Figure 8** presents the integrated human health risk assessment of heavy metals in urban soils using hazard quotient (HQ), hazard index (HI), and carcinogenic risk (CR) indicators for children and adults. Nevertheless, children consistently exhibit higher HI values than adults, reflecting their greater vulnerability, primarily due to lower body weight and higher soil ingestion rates.

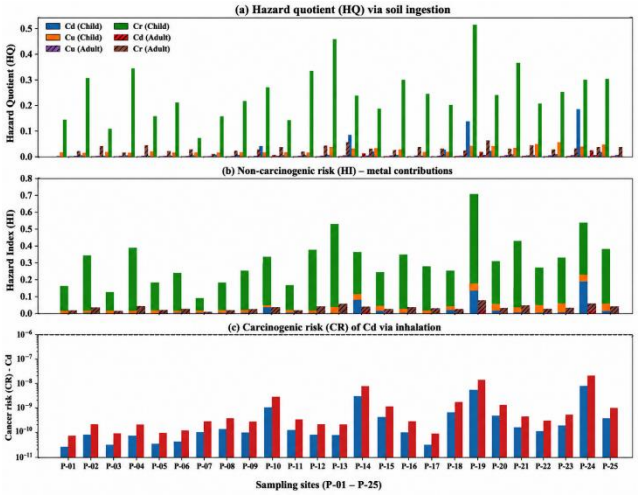


Figure 8. Presents the integrated human health risk assessment of heavy metals in urban soils using hazard quotient (HQ), hazard index (HI), and carcinogenic risk (CR) indicators for children and adults

As shown in Figure 8(a), hazard quotient (HQ) values for individual metals (Cd, Cu, and Cr) via soil ingestion were consistently below the safety threshold (HQ = 1) at all sampling sites. The highest HQ values were observed for chromium (Cr) in children, reaching approximately 0.52, whereas cadmium (Cd) and copper (Cu) exhibited substantially lower HQ values, generally <0.20 and <0.05, respectively. Across all sites, children consistently displayed higher HQ values than adults, reflecting their greater exposure potential associated with higher soil ingestion rates and lower body weight.

Figure 8(b) presents the cumulative non-carcinogenic risk expressed as the hazard index (HI). All calculated HI values remained below unity (HI < 1), indicating that adverse non-carcinogenic health effects are unlikely under current exposure conditions. The maximum HI value, approximately 0.70, was recorded for children at the most impacted site, whereas adult HI values did not exceed 0.10.

Chromium (Cr) accounted for the largest numerical contribution to the calculated HI (approximately 60–75%), followed by Cd (15–30%) and Cu (<10%). These relative contributions arise from the HHRA calculation framework, which combines measured concentrations with toxicological reference values and exposure parameters, and therefore should be interpreted as quantitative estimates of potential health risk rather than independent evidence of contaminant sources or environmental significance.

Although cadmium contributed a smaller proportion to the calculated HI, the measured Cd concentrations exhibited the greatest enrichment relative to background values and the most pronounced spatial clustering (sites P-14, P-19, and P-24). Consequently, Cd remains the principal contaminant of environmental concern based on its measured concentrations, spatial distribution, and contamination indices, whereas the calculated HHRA metrics quantify the potential health risks associated with these measured concentrations.

Carcinogenic risk associated with cadmium inhalation is illustrated in Figure 8(c). Estimated CR values ranged from approximately 2×10^{-11} to 3×10^{-9} for children and from 5×10^{-11} to 7×10^{-9} for adults, remaining several orders of magnitude below the acceptable risk level of 10^{-6} recommended by international guidelines. Although adults exhibited slightly higher CR values due to longer exposure duration, all estimates fall within the negligible risk range, indicating no significant lifetime cancer risk related to Cd inhalation.

The HQ, HI, and CR values reported in this study are mathematical outputs derived from the measured concentrations together with the exposure assumptions and toxicological reference values adopted in the HHRA model. Accordingly, these indicators are used to quantify potential health risks under the assumed exposure scenarios and should not be interpreted as independent validation of the contamination assessment.

From a soil management and policy perspective, these findings emphasize the importance of preventive and risk-based strategies rather than immediate remediation. Industrial and high-traffic areas identified as Cd contamination hotspots should be prioritized for regular monitoring, emission control, and land-use management. Measures aimed at reducing direct human–soil contact, together with long-term soil quality monitoring, are recommended to prevent future increases in exposure.

Overall, the measured concentrations, their spatial distribution, and the calculated HHRA indicators collectively indicate that heavy metal contamination in the studied urban soils does not pose significant non-carcinogenic or carcinogenic health risks for either children or adults under the current exposure scenarios. Nevertheless, the consistently higher calculated risk indicators for children, together with the strong spatial enrichment of cadmium, underscore the importance of continuous monitoring and preventive urban soil management, particularly in areas subject to intense anthropogenic pressures.

5. Multivariate analysis of heavy metal contamination (PCA and HCA)

The combined principal component analysis (PCA) and hierarchical cluster analysis (HCA) quantitatively elucidate contamination patterns and potential sources of heavy metals in the urban soils of Annaba City. PCA indicates that the first two principal components explain 79.2% of the total variance, with Dim1 accounting for 57.1% and Dim2 for 22.1%, demonstrating that these axes effectively summarize the main structure of the dataset (**Figure 9**).

As illustrated in the PCA biplot (**Figure 9a**), sampling sites are clearly separated into three groups reflecting different

contamination characteristics. Dim1 is characterized by strong positive loadings of cadmium (Cd) and chromium (Cr), indicating their dominant contribution to overall variance. Sites with high negative scores along Dim1 correspond to locations exhibiting elevated metal concentrations (Cd up to 14.01 mg·kg^{-1}; Cr up to 121.24 mg·kg^{-1}) and high contamination indices (CF_Cd up to 144.43; Igeo_Cd up to 6.59). These sites spatially coincide with industrial zones, suggesting a major influence of metallurgical and industrial emissions. In contrast, sites located on the positive side of Dim1 display substantially lower metal concentrations (Cd < 0.5 mg·kg^{-1}; Cr < 70 mg·kg^{-1}) and represent background or weakly impacted conditions. An intermediate group occupies a transitional position, indicating moderate contamination levels.

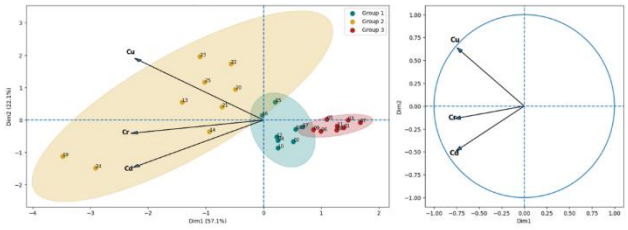


Figure 9. Principal component analysis (PCA) of heavy metals in urban soils showing (a) the biplot of sampling sites grouped into three clusters and (b) the correlation circle of Cd, Cu, and Cr.

Dim2 is mainly controlled by copper (Cu), with concentrations ranging from 30.56 to 152.17 mg·kg^{-1} and contamination factors (CF_Cu) reaching up to 6.73. The separation along Dim2 (Figure 9b) highlights a distinct contamination pathway for Cu, likely related to traffic emissions and agricultural inputs rather than dominant industrial sources.

Hierarchical cluster analysis (HCA) further supports the PCA interpretation by grouping the 25 sampling sites into three main clusters based on Cd, Cu, and Cr concentrations using Ward's linkage method and Euclidean distance (Figure 11). One cluster group highly contaminated industrial site, notably P-14, P-19, and P-24, characterized by very high Cd concentrations (6.08–14.01 mg·kg^{-1}) and extreme contamination factors (CF_Cd > 60). A second cluster includes moderately contaminated sites with mixed metal signatures (Cd = 0.5–2.6 mg·kg^{-1}; Cu = 50–110 mg·kg^{-1}), while a third cluster comprises background sites with relatively low metal concentrations (Cd < 0.4 mg·kg^{-1}; Cu < 50 mg·kg^{-1}; Cr generally < 70 mg·kg^{-1}).

The strong consistency between PCA loadings (Figure 9) and HCA clustering (Figure 10) confirms the robustness of the multivariate interpretation. Although chromium contributes significantly to the statistical variance and to the numerical structure of the hazard index, cadmium shows the strongest association with contamination hotspots, enrichment indices, and industrial clusters. This quantitative multivariate evidence supports the identification of cadmium as the primary contaminant of environmental concern in Annaba urban soils, with copper and chromium playing secondary roles linked to traffic-related and largely geogenic influences, respectively.

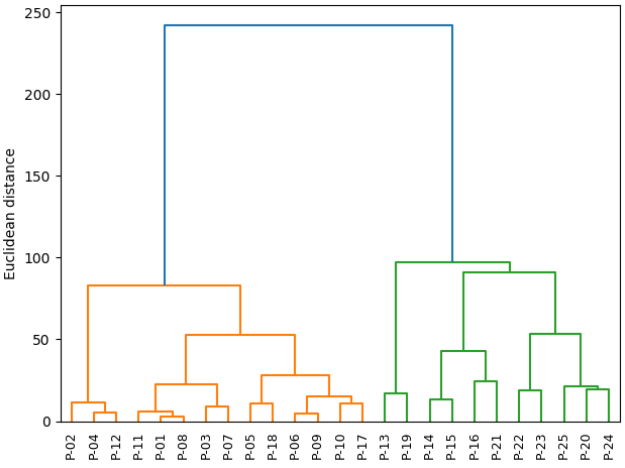


Figure 10. Hierarchical cluster analysis (HCA) dendrogram of urban soil samples based on Cd, Cu, and Cr concentrations using Ward's linkage method and Euclidean distance.

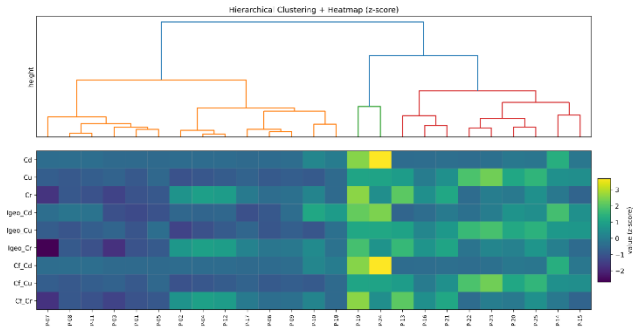


Figure 11. Hierarchical Clustering and Z-Score Heatmap of Heavy Metals (Cd, Cu, Cr) and Associated Contamination Indices (Igeo and CF) Across Sampling Sites

Hierarchical clustering combined with z-score–normalized heatmap analysis revealed a clear geochemical differentiation among the studied samples (P01–P25), delineating two principal clusters characterized by distinct contamination signatures. Cadmium (Cd) emerged as the primary discriminating factor between these clusters, exhibiting markedly elevated standardized values in one group, consistently reflected in its geoaccumulation index (Igeo-Cd) and contamination factor (CF-Cd). This strong concordance between measured concentrations and derived indices highlights the robustness and internal consistency of the contamination assessment framework in Figure 11.

In contrast, copper (Cu) demonstrated moderate enrichment trends, whereas chromium (Cr) showed a more heterogeneous spatial distribution, suggesting a potential mixed lithogenic–anthropogenic origin. The pronounced separation of clusters at higher linkage distances indicates substantial geochemical heterogeneity, likely driven by spatially variable anthropogenic inputs rather than uniform natural background conditions.

Overall, the multivariate structure of the dataset clearly identifies Cd as the principal driver of contamination variability and a reliable tracer of localized pollution sources within the investigated area.

6. Correlation Analysis and Integrated Spatial–Statistical Interpretation

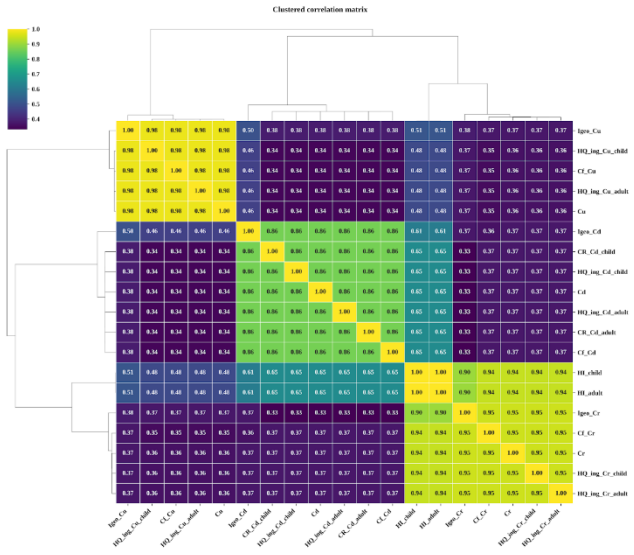


Figure 12. Clustered correlation matrix linking heavy metal concentrations (Cd, Cu, Cr), pollution indices (I*geo*, CF), and human health risk indicators (HQ, HI, and CR) for children and adults in urban soils.

The clustered correlation matrix highlights the relationships between heavy metal concentrations (Cd, Cu, and Cr), pollution indices (I*geo* and CF), and human health risk indicators (HQ, HI, and CR) for both children and adults (Figure 12). Cadmium (Cd) exhibits very strong correlations with its contamination indices (I*geo*_Cd: r = 0.86; CF_Cd: r = 1.00) and with carcinogenic risk via inhalation (CR_Cd: r = 0.87–0.91), indicating that Cd enrichment is closely linked to increased potential health risk. In contrast, copper (Cu) and chromium (Cr) show weaker correlations with health risk indicators (r = 0.34–0.57).

Although non-carcinogenic risk values for all metals remain below the safety threshold for both children and adults (HQ < 1; HI < 1), children consistently display stronger correlations between Cd concentrations and both HQ and HI values (r ≈ 0.78) compared to adults (r ≈ 0.55), reflecting their greater susceptibility. This increased sensitivity in children is not solely attributable to physiological differences, such as lower body weight, but is also driven by behavioral exposure pathways, particularly frequent hand-to-mouth activity and higher incidental ingestion of contaminated soil and dust during outdoor play, which enhance overall exposure intensity. While calculated carcinogenic risks for Cd remain within acceptable limits (CR < 10^{-6}), their strong association with Cd enrichment indices suggests that localized accumulation may represent a potential long-term environmental concern rather than an immediate health risk.

Pairwise relationships between heavy metal concentrations and health risk indicators further support these observations (Figure 13). Cadmium shows the strongest associations with both non-carcinogenic (HQ) and carcinogenic (CR) risk indicators, whereas Cu and Cr exhibit more moderate and diffuse relationships, consistent with their lower enrichment levels and more uniform spatial distributions.

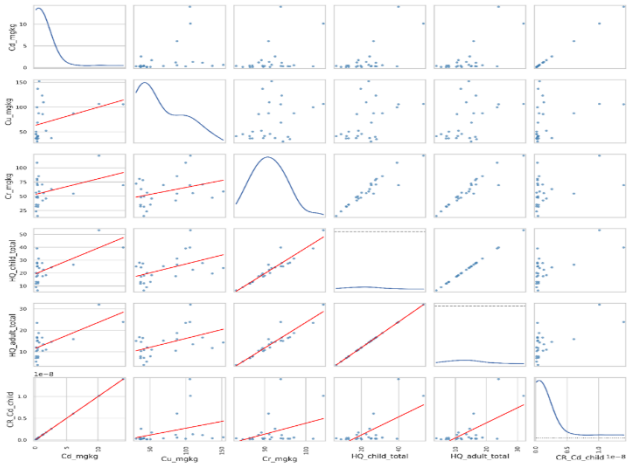


Figure 13. Pairwise relationships between heavy metal concentrations (Cd, Cu, Cr) and human health risk indicators (HQ and CR) for different age groups in urban soils.

An integrated spatial–statistical interpretation reveals pronounced cadmium hotspots in the southern and southeastern sectors of the study area, where concentrations reach 10.15–14.01 mg·kg^{-1}, exceeding the background value (0.097 mg·kg^{-1}) by more than two orders of magnitude. These hotspots spatially coincide with elevated non-carcinogenic risk indicators for children, with HQ values approaching—but not exceeding—the regulatory threshold (HQ_child ≈ 0.7–0.9). Principal component analysis corroborates this pattern, with PC1 explaining 57.1% of the total variance and showing strong loadings of Cd together with pollution and risk indicators.

In contrast, copper and chromium load more weakly on PC1 and exhibit only moderate correlations with HQ values (r = 0.34–0.57), indicating a secondary contribution to overall health risk. Although chromium contributes numerically to the hazard index due to its toxicological reference values, its relatively weak enrichment and spatial uniformity suggest a more limited environmental concern compared to cadmium. Overall, the combined spatial, correlation, and multivariate evidence indicates a source-driven contamination pattern dominated by industrial Cd emissions, with additional contributions from traffic-related activities and intensive agricultural fertilization.

7. Conclusions

This study provides an integrated assessment of cadmium (Cd), copper (Cu), and chromium (Cr) in urban surface soils (0–5 cm) of Annaba City, combining pollution indices (CF and I*geo*), GIS-based spatial analysis, human health risk assessment (HHRA), and multivariate statistical approaches.

Overall, Cd is identified as the primary contaminant of concern, showing pronounced hotspot enrichment near industrial zones, particularly the El Hadjar steel complex Although HHRA results indicate that both non-carcinogenic and carcinogenic risks currently remain within acceptable limits, children consistently exhibit higher exposure levels

than adults, highlighting increased vulnerability to soil-associated contaminationFrom a management perspective, the findings support a shift from descriptive assessment toward risk-based environmental governance. Priority attention should be given to Cd hotspot areas through continuous monitoring systems capable of tracking temporal changes and supporting early-warning decision-making. Risk-informed land-use planning is recommended, including restrictions on sensitive uses such as playgrounds, schools, and childcare facilities near highly contaminated sites (e.g., Site P-24). Exposure mitigation strategies should include reducing direct soil–human contact and limiting resuspension of contaminated dust. Public awareness programs should discourage home vegetable cultivation in metal-enriched soils to minimize cadmium transfer through the food chain.

At the industrial governance level, strengthening emission control at the source through cleaner production technologies and stricter compliance mechanisms remains essential. These measures should be complemented by the integration of Environmental, Social, and Governance (ESG) frameworks within major industrial zones such as the El Hadjar steel complex, improving transparency and corporate accountability in emission reporting (Yan *et al.*, 2025).

Long-term soil monitoring programs are essential to evaluate contamination dynamics, assess mitigation effectiveness, and support adaptive environmental management strategies in rapidly urbanizing regions.

Finally, while this study is based on total metal concentrations, future research should incorporate chemical speciation analysis, particularly for chromium, to distinguish between Cr(III) and Cr(VI). This distinction is essential for accurately characterizing toxicity, mobility, and bioavailability, thereby improving exposure assessment and strengthening risk-informed environmental decision-making.

Acknowledgement

The authors gratefully acknowledge the financial support provided by the Ministry of Higher Education and Scientific Research and the General Directorate for Scientific and Technological Development (Algeria).

Disclosure statement

No potential conflict of interest was reported by the author(s).

Funding

This study was supported by the Ministry of Higher Education and Scientific Research of Algeria, as well as the General Directorate of Scientific and Technological Development, Algeria, for their financial support.

Ethical considerations

This study does not require ethical approval as it does not involve any animal or human subjects, nor does it require informed consent.

Data availability statement

The datasets generated and/or analyzed during this study are available from the corresponding author upon reasonable request.

Authorship Contributions

Seifeddine SELLAMI: Conceptualization; Methodology; Investigation; Data curation; Formal analysis; Writing – Original Draft; Writing – Review & Editing; Ahmed Abderrahim YAHIAOUI: Investigation; Sampling; Laboratory analysis; Data curation; Said LIFA: Formal analysis; Validation; Visualization; Omar TEBBOUB: Methodology; Software; Statistical analysis; Data interpretation; Ali HADJELA: Resources; Field supervision; Data validation; Fares ZAAMOUCHE: Laboratory analysis; Quality control; Validation; Redouane LEMOUI: Data interpretation; Visualization; Writing – Review & Editing; Lotfi BENMEKHBI: Supervision; Project administration; Writing – Review & Editing; Ouahida ZEGHOUAN: Conceptualization; Supervision; Funding acquisition; Final approval of the manuscript.

References

Abraham, J., Dowling, K., Florentine, S. (2018). Assessment of potentially toxic metal contamination in the soil of a legacy mine site in Central Victoria, Australia. Chemosphere, 192: 122–132. https://doi.org/10.1016/j.chemosphere.2017.10.150

AFNOR. (1992). Qualité des sols — Préparation d'un échantillon de sol pour analyse physico-chimique: Séchage, émottage et tamisage à 2 mm (NF X31-101). Association Française de Normalisation, Paris.

AFNOR. (2005). Soil quality — Determination of pH (NF ISO 10390:2005). International Organization for Standardization.

Ahmad, W., Alharthy, R.D., Zubair, M. (2021). Toxic and heavy metals contamination assessment in soil and water to evaluate human health risk. Scientific Reports, 11: 17006. https://doi.org/10.1038/s41598-021-94616-4

Aksouh, M. Y., Boudieb, N., Benosmane, N., Moussaoui, Y., Michalski, R., Klyta, J., & Kończyk, J. (2024). Presence of Heavy Metals in Irrigation Water, Soils, Fruits, and Vegetables: Health Risk Assessment in Peri-Urban Boumerdes City, Algeria. Molecules, 29(17), 4187.

Alhadi, Z., Munaf, E. (2024). Environmental quality analysis from the perspective of infrastructure development and investment policy in Indonesia. International Journal of Environmental Impacts, 7(3): 543–559. https://doi.org/10.18280/ijei.070316

Amiard, J.C., Pineau, A., Boiteau, H.L., Metayer, C., Amiard-Triquet, C. (1987). Application of atomic absorption spectrophotometry using Zeeman effect to the determination of eight trace elements (Ag, Cd, Cr, Cu, Mn, Ni, Pb, and Se) in biological materials. Water Research, 21: 693–697. https://doi.org/10.1016/0043-1354(87)90081-9

Arab, L.H., Boutaleb, A., Berdous, D. (2021). Environmental assessment of heavy metal pollution in the polymetallic district of Kef Oum Teboul (El Kala, Northeast Algeria). Environmental Earth Sciences, 80(7): 277. https://doi.org/10.1007/s12665-021-09570-1

Aubert, G. (1978). Méthodes d'analyses des sols. C.R.D.P., Marseille: 123–127.

Awadh, S.M., Al-Kelabi, J.A. (2016). Assessment of groundwater quality using water quality index in Al-Hawija area, Northern Iraq. Iraqi Geological Journal, 39–49(1): 67–76. https://doi.org/10.46717/igj.39-49.1.5Ms-2016-06-27

Ayaz, H., Nawaz, R., Nasim, I., Irshad, M.A., Irfan, A., Khurshid, I., Okla, M.K., Wondmie, G.F., Ahmed, Z., Bourhia, M. (2023). Comprehensive human health risk assessment of heavy metal contamination in urban soils: Insights from selected metropolitan zones. Frontiers in Environmental Science, 11: 1260317. https://doi.org/10.3389/fenvs.2023.1260317

Baran, A., Wieczorek, J. (2015). Application of geochemical and ecotoxicity indices for assessment of heavy metals content in soils. Archives of Environmental Protection, 41(2): 53–62. https://doi.org/10.1515/aep-2015-0019

Bartoszek, L., Gruca-Rokosz, R., Pękala, A., Czarnota, J. (2022). Heavy metal accumulation in sediments of small retention reservoirs—Ecological risk and the impact of humic substances distribution. Resources, 11(12): 113. https://doi.org/10.3390/resources11120113

Benselhoub, A., Kharytonov, M., Bouabdallah, S., Bounouala, M., Idres, A., & Boukelloul, M. L. (2015). Bioecological assessment of soil pollution with heavy metals in Annaba (Algeria). Studia Universitatis "Vasile Goldiş", Seria Ştiinţele Vieţii, 25(1), 17–22.

Bi, C., Zhou, Y., Chen, Z., Jia, J., Bao, X. (2018). Heavy metals and lead isotopes in soils, road dust and leafy vegetables and health risks via vegetable consumption in the industrial areas of Shanghai, China. Science of the Total Environment, 619–620: 1349–1357. https://doi.org/10.1016/j.scitotenv.2017.11.177

Bołzan, B.D. (2017). Effect of pH and soil environment. World News of Natural Sciences, 8: 50–60.

Cai, K., Li, C., Song, Z., Gao, X., Wu, M. (2019). Pollution and health risk assessment of carcinogenic elements As, Cd, and Cr in multiple media—A case of a sustainable farming area in China. Sustainability, 11(19): 5208. https://doi.org/10.3390/su11195208

CEPA (China Environmental Protection Administration). (1995). Environmental Quality Standard for Soils, GB 15618-1995. Beijing: China Environmental Science Press.

Chen, T., Wen, X., Zhou, J., Lu, Z., Li, X., Yan, B. (2023). A critical review on the migration and transformation processes of heavy metal contamination in lead-zinc tailings of China. Environmental Pollution, 338: 122667. https://doi.org/10.1016/j.envpol.2023.122667

Chen, Y.G., He, X.L., Huang, J.H., Luo, R., Ge, H.Z., Wołowicz, A., Wawrzkiewicz, M.,

Chileshe, M.N., Syampungani, S., Festin, E.S., Tigabu, M., Daneshvar, A., Odén, P.C. (2020). Physico-chemical characteristics and heavy metal concentrations of copper mine wastes in Zambia: Implications for pollution risk and restoration. Journal of Forestry Research, 31(4): 1283–1293. https://doi.org/10.1007/s11676-019-00921-0

China General Environmental Monitoring Station. (1990). Background values of elements in soils of China. China Environmental Science Press, Beijing.

Chinese Environmental Protection Administration. (1995). Environmental quality standard for soils (GB 15618-1995). Beijing.

Gładysz-Płaska, A., Li, B., Yu, Q.X., Kołodyńska, D., Lv, G.Y., Chen, S.H. (2021). Impacts of heavy metals and medicinal crops on ecological systems, environmental pollution, cultivation, and production processes in China. Ecotoxicology and Environmental Safety, 219: 112336. https://doi.org/10.1016/j.ecoenv.2021.112336

Diang, M., Li, Y., Yang, J., Lei, K., Li, F., Zheng, D., Fang, X., Cao, Y. (2021). Heavy metal contamination risk assessment and correlation analysis of heavy metal contents in soil and crops. Environmental Pollution, 278: 116911. https://doi.org/10.1016/j.envpol.2021.116911

Ejaz, U., Khan, S.M., Shah, S.F.A., Khalid, N., Jehangir, S., Rizvi, Z.F., Svenning, J.-C. (2025). Integrative data-driven analytics for assessing ecological and human health risks of soil heavy metal contamination. Journal of Hazardous Materials Advances, 17: 100596. https://doi.org/10.1016/j.hazadv.2025.100596

El Zrelli, R., Courjault-Radé, P., Rabaoui, L., Castet, S., Michel, S., Bejaoui, N. (2015). Heavy metal contamination and ecological risk assessment in the surface sediments of the coastal area surrounding the industrial complex of Gabes City, Gulf of Gabes, SE Tunisia. Marine Pollution Bulletin, 101(2): 922–929. https://doi.org/10.1016/j.marpolbul.2015.10.047

Gautam, K., Sharma, P., Dwivedi, S., Singh, A., Gaur, V.K., Varjani, S., Srivastava, J.K., Pandey, A., Chang, J.-S., Ngo, H.H. (2023). A review on control and abatement of soil pollution by heavy metals: Emphasis on artificial intelligence in recovery of contaminated soil. Environmental Research, 225: 115592. https://doi.org/10.1016/j.envres.2023.115592

Goher, M.E., Ali, M.H.H., El-Sayed, S.M. (2019). Heavy metals contents in Nasser Lake and the Nile River, Egypt: An overview. Egyptian Journal of Aquatic Research, 45(4): 301–312. https://doi.org/10.1016/j.ejar.2019.12.002

Golia, E.E., Tsiropoulos, G.N., Füleky, G., Floras, S., Vleioras, S. (2019). Pollution assessment of potentially toxic elements in soils of different taxonomy orders in Central Greece. Environmental Monitoring and Assessment, 191(2): 106. https://doi.org/10.1007/s10661-019-7201-1

Goncharov, G., Soktoev, B., Farkhutdinov, I., Matveenko, I. (2024). Heavy metals in urban soil: Contamination levels, spatial distribution and human health risk assessment (the case of Ufa city, Russia). Environmental Research, 257: 119216. https://doi.org/10.1016/j.envres.2024.119216

Gujre, N., Rangan, L., Mitra, S. (2021). Occurrence, geochemical fraction, ecological and health risk assessment of cadmium, copper and nickel in soils contaminated with municipal solid wastes. Chemosphere, 271: 129573. https://doi.org/10.1016/j.chemosphere.2021.129573

Guo, G., Zhang, D., Wang, Y. (2021). Source apportionment and source-specific health risk assessment of heavy metals in size-fractionated road dust from a typical mining and smelting area, Gejiu, China. Environmental Science and Pollution Research, 28: 9313–9326. https://doi.org/10.1007/s11356-020-11312-y

Guo, Y.G., Li, Q., Guo, Y.P. (2016). Metals in exposed-lawn soils from 18 urban parks and its human health implications in southern China's largest city, Guangzhou. Journal of Cleaner Production, 115: 122–129. https://doi.org/10.1016/j.jclepro.2015.12.031

Hadif, W.M., Abd Rahim, S., Sahid, I. (2020). Assessment of heavy metal pollution using the Geo-accumulation Index (I-Geo),

Pollution Load Index (PLI) and Potential Ecological Risk Index (RI) in paddy field soils adjacent to ultrabasic soils. University of Thi-Qar Journal of Agricultural Research, 9(1): 85–97. https://doi.org/10.54174/utjagr.v9i1.108

Hafiane Hedahdia, I., Boukhemis, K. (2024). Appraisal of knowledge and attitudes of local people towards importance of conservation of the archaeological heritage: Case of the Hippone site in Annaba (Algeria). Journal of Cultural Heritage Management and Sustainable Development. https://doi.org/10.1108/jchmsd-08-2023-0132

Islam, M.S., Ismail, Z., Jamal, M.H., Ibrahim, Z., Jumain, M., Islam, A.R.M.T., Idris, A.M. (2022). Heavy metals from different land use soil in the capital of Ancient Pundranagar, Bangladesh: A preliminary study for ecological risk assessment. Chemistry and Ecology, 38(8): 720–743. https://doi.org/10.1080/02757540.2022.2100360

Istanbullu, S.N., Sevik, H., Isinkaralar, K. (2023). Spatial distribution of heavy metal contamination in road dust samples from an urban environment in Samsun, Türkiye. Bulletin of Environmental Contamination and Toxicology, 110: 78. https://doi.org/10.1007/s00128-023-03720-w

Jiang, H., Cai, L., Hu, G., Wen, H., Luo, J., Xu, H., Chen, L. (2021). An integrated exploration on health risk assessment quantification of potentially hazardous elements in soils from the perspective of sources. Ecotoxicology and Environmental Safety, 208: 111489. https://doi.org/10.1016/j.ecoenv.2020.111489

Khalili, R., Zali, A., Motaghi, H. (2021). Evaluation of heavy metals in water and sediments of Haraz River, using Pollution Load Index (PLI) and Geoaccumulation Index (Igeo). Iranian Journal of Soil and Water Research, 52(4): 933–942. https://doi.org/10.22059/ijswr.2021.316080.668850

Koleayo, O.O., Raimi, M.O., Waleola, T.O. (2021). Public health knowledge and perception of microplastics pollution: Lessons from the Lagos Lagoon. Research Square (Preprint, Version 1). https://doi.org/10.21203/rs.3.rs-506361/v1

Ksiezopolska, A. (2002). Physico-chemical characterization of organic-mineral complexes. Institute of Agrophysics, Polish Academy of Sciences, Lublin.

Kurniawan, E., Syifauddin, M., Sholeh, M., Sriyanto, Sari, S.N. (2024). Environmental problem-solving learning model with geographic information system-based learning media. International Journal of Environmental Impacts, 7(3): 381–394. https://doi.org/10.18280/ijei.070301

Liang, J., Liu, Z., Tian, Y., Shi, H., Fei, Y., Qi, J., Mo, L. (2023). Research on health risk assessment of heavy metals in soil based on multi-factor source apportionment: A case study in Guangdong Province, China. Science of the Total Environment, 858(3): 159991. https://doi.org/10.1016/j.scitotenv.2022.159991

Lifa, S., Sellami, S., Zeghouan, O., Tebboub, O., & Zaamouche, F. (2025). Analyzing soil pollution: Heavy metals in Setif City region using ICP-OES technique. International Journal of Environmental Impacts, 8(6), 1152–1166. https://doi.org/10.56578/ijei080604

Lu, S.G., Bai, S.Q. (2010). Contamination and potential mobility assessment of heavy metals in urban soils of Hangzhou, China: Relationship with different land uses. Environmental Earth Sciences, 60: 1481–1490. https://doi.org/10.1007/s12665-009-0283-2

Luo, X.-S., Ding, J., Xu, B., Wang, Y.-J., Li, H.-B., Yu, S. (2012). Incorporating bioaccessibility into human health risk assessments of heavy metals in urban park soils. Science of the Total Environment, 424: 88–96. https://doi.org/10.1016/j.scitotenv.2012.02.053

Ma, S., H. Zeng, H. Yan, and D. Li. (2025). "Clear Waters, Flourishing Growth: Decoupling Water Pollution From Economic Growth in Shanxi Province, China." Water Environment Research97, no. 12: e70231. https://doi.org/10.1002/wer.70231

Maas, S., Scheifler, R., Benslama, M., Crini, N., Lucot, E., Brahmia, Z., Benyacoub, S., Giraudoux, P. (2010). Spatial distribution of heavy metal concentrations in urban, suburban and agricultural soils in a Mediterranean city of Algeria. Environmental Pollution, 158: 2294–2301. https://doi.org/10.1016/j.envpol.2010.02.001

Mameri, Y., Belattar, S., Seraghni, N., Debbache, N., Sehili, T. (2024). Powdered activated carbon adsorbent for Eosin Y removal: Modeling of adsorption isotherm data, thermodynamic and kinetic studies. International Journal of Chemical Reactor Engineering, 22(2): 189–197. https://doi.org/10.1515/ijcre-2023-0074

McKone, T.E., Daniels, J.I. (1991). Estimating human exposure through multiple pathways from air, water, and soil. Regulatory Toxicology and Pharmacology, 13(1): 36–61. https://doi.org/10.1016/0273-2300(91)90040-3

Men, C., Liu, R., Xu, L., Wang, Q., Guo, L., Miao, Y., Shen, Z. (2020). Source-specific ecological risk analysis and critical source identification of heavy metals in road dust in Beijing, China. Journal of Hazardous Materials, 388: 121763. https://doi.org/10.1016/j.jhazmat.2019.121763

Miletić, A., Lučić, M., Onjia, A. (2023). Exposure factors in health risk assessment of heavy metal(loid)s in soil and sediment. Metals, 13(7): 1266. https://doi.org/10.3390/met130712466

Mohammad Khalil, R. K., Solangi, K. A., Bala Alhassan, A., Razzaq Khan, W., & Othman Aljahdali, M. (2024). Heavy Metals Distribution in Mangrove Leaves in Various Sudanese Coastal Zones at The Red Sea. Global NEST Journal, 26(10), 1–9. https://doi.org/10.30955/gnj.06619"

Müller, G. (1969). Index of geoaccumulation in sediments of the Rhine River. GeoJournal, 2(3): 108–118.

Nasir, M.J., Wahab, A., Ayaz, T. (2023). Assessment of heavy metal pollution using contamination factor, pollution load index, and geoaccumulation index in Kalpani River sediments, Pakistan. Arab Journal of Geosciences, 16: 143. https://doi.org/10.1007/s12517-023-11231-5

Pan, Y., Chen, M., Wang, X., Chen, Y. (2024). Ecological risk, source apportionment, and influencing factors of heavy metals in soil in a typical lead-zinc mining watershed, Guangxi, China. Journal of Environmental Chemical Engineering, 12(3): 112731. https://doi.org/10.1016/j.jece.2024.112731

Peña-Fernández, A., González-Muñoz, M.J., Lobo-Bedmar, M.C. (2014). Establishing the importance of human health risk assessment for metals and metalloids in urban environments. Environment International, 72: 176–185. https://doi.org/10.1016/j.envint.2014.04.007

Poggio, L., Višcaj, B., Hepperle, E., Schulin, R., Marsan, F.A. (2008). Introducing a method of human health risk evaluation for planning and soil quality management of heavy metal-polluted soils—An example from Grugliasco (Italy). Landscape

and Urban Planning, 88: 64–72. https://doi.org/10.1016/j.landurbplan.2008.08.002

Qi, Z., Gao, X., Qi, Y., Li, J. (2020). Spatial distribution of heavy metal contamination in Mollisol dairy farm. Environmental Pollution, 12(3): 114621. https://doi.org/10.1016/j.envpol.2020.114621

Qiao, P., Wang, S., Li, J., Zhao, Q., Wei, Y., Lei, M., Yang, J., Zhang, Z. (2023). Process, influencing factors, and simulation of the lateral transport of heavy metals in surface runoff in a mining area driven by rainfall: A review. Science of the Total Environment, 857: 159119. https://doi.org/10.1016/j.scitotenv.2022.159119

Qing, X., Yutong, Z., Shenggao, L. (2015). Assessment of heavy metal pollution and human health risk in urban soils of steel industrial city (Anshan), Liaoning, Northeast China. Ecotoxicology and Environmental Safety, 120: 377–385. https://doi.org/10.1016/j.ecoenv.2015.06.019

Radi, N., Hirche, A., Boutaleb, A. (2023). Assessment of soil contamination by heavy metals and arsenic in Tamesguida abandoned copper mine area, Médéa, Algeria. Environmental Monitoring and Assessment, 195: 247. https://doi.org/10.1007/s10661-022-10862-7

Raimi, M.O., Izah, S.C. (2022). Leaving no one behind: Impact of soil pollution on biodiversity in the Global South: A global call for action. Biodiversity in Africa: Potentials, Threats and Conservation, Sustainable Development and Biodiversity, 29. Springer, Singapore. https://doi.org/10.1007/978-981-19-3326-4_8

Raimi, O.M., Sawyerr, O.H., Ezekwe, C.I., Gabriel, S. (2022). Many oil wells, one evil: Comprehensive assessment of toxic metals concentration, seasonal variation, and human health risk in drinking water quality in areas surrounding crude oil exploration facilities in Rivers State, Nigeria. International Journal of Hydrology, 6(1): 23–42. https://doi.org/10.15406/ijh.2022.06.00299

Saadat, S. (2022). Evaluating sediment pollution using contamination indices and risk assessment in mineralized zones, Eastern Iran. Journal of Mining and Environment, 13(4): 1239–1253. https://doi.org/10.22044/jme.2023.13781.2559

Salhi, Z., Dönmez, Y. (2021). Urban identity and environmental perception in Annaba, Algeria. Kastamonu University Journal of Engineering Sciences, 7(2): 83–99.

Seifi, M., Mahvi, A.H., Hashemi, S.Y., Arfaeinia, H., Pasalari, H., Zarei, A., Changani, F. (2019). Spatial distribution, enrichment and geo-accumulation of heavy metals in surface sediments near urban and industrial areas in the Persian Gulf. Desalination and Water Treatment, 158: 130–139. https://doi.org/10.5004/dwt.2019.24238

Sellami, S., Zeghouan, O., Dhahri, F., Mechi, L., Moussaoui, Y., & Kebabi, B. (2022). Assessment of heavy metal pollution in urban and peri-urban soil of Setif city (High Plains, eastern Algeria). Environmental Monitoring and Assessment, 194, 126. https://doi.org/10.1007/s10661-022-09781-4

Shukla, A.K., Pradhan, M., Tiwari, O.N. (2024). Heavy metal contamination of surface sediments–soil adjoining the largest copper mine waste dump in Central India using multivariate pattern recognition techniques and geo-statistical mapping. Nature Environment and Pollution Technology, 23(3): 1363–1374. https://doi.org/10.46488/NEPT.2024.v23i03.009

Strenge, D.L., Chamberlain, P.J. (1995). Multimedia Environmental Pollutant Assessment System (MEPAS®): Exposure pathway and human health impact assessment models. Technical Report, OSTI. https://doi.org/10.2172/70754

Sun, X., Zhang, L., Lv, J. (2021). Spatial assessment models to evaluate human health risk associated to soil potentially toxic elements. Environmental Pollution, 268(B): 115699. https://doi.org/10.1016/j.envpol.2020.115699

Szczepanik, M., Szyszlak-Bargłowicz, J., Zając, G., Koniuszy, A., Hawrot-Paw, M., Wolak, A. (2021). The use of multivariate data analysis (HCA and PCA) to characterize ashes from biomass combustion. Energies, 14(21): 6887. https://doi.org/10.3390/en14216887

Thavamani, P., Megharaj, M., Naidu, R. (2012). Multivariate analysis of mixed contaminants (PAHs and heavy metals) at manufactured gas plant site soils. Environmental Monitoring and Assessment, 184: 3875–3885. https://doi.org/10.1007/s10661-011-2230-4

Tong, S., Li, H., Wang, L., Tudi, M., Yang, L. (2020). Concentration, spatial distribution, contamination degree and human health risk assessment of heavy metals in urban soils across China between 2003 and 2019—A systematic review. International Journal of Environmental Research and Public Health, 17(9): 3099. https://doi.org/10.3390/ijerph17093099

U.S. EPA. (2007). Method 3051A (SW-846): Microwave assisted acid digestion of sediments, sludges, soils, and oils (Revision 1). United States Environmental Protection Agency, Washington, DC.

Umwanzisiwemuremyi, O., Abidin, Z., Setiawan, Y. (2024). Spatial assessment of illegal plastic waste dumping and environmental impacts in Babakan and Cikarawang in Bogor regency. International Journal of Environmental Impacts, 7(2): 293–303. https://doi.org/10.18280/ijei.070214

USDA. (1998). Soil Quality Indicators: pH. Natural Resources Conservation Service, United States Department of Agriculture.

Uwizeyimana, H., Wang, M., Chen, W., Khan, K. (2017). The eco-toxic effects of pesticide and trace metal mixtures towards earthworms in soil. Environmental Toxicology and Pharmacology, 55: 20–29. https://doi.org/10.1016/j.etap.2017.08.001

Wang, X., Wei, N., Ji, G., Liu, R., Huang, G., Zhang, H. (2022). Assessment of the driving pollution factors of soil environmental quality based on China's risk control standard: Multiple big data-based approaches with intensive sampling. International Journal of Environmental Research and Public Health, 19(19): 12459. https://doi.org/10.3390/ijerph191912459

Wei, B., Yu, J., Cao, Z., Meng, M., Yang, L., Chen, Q. (2020). The availability and accumulation of heavy metals in greenhouse soils associated with intensive fertilizer application. International Journal of Environmental Research and Public Health, 17(15): 5359. https://doi.org/10.3390/ijerph17155359

Xiao, M., Qian, L., Yang, B., Zeng, G., Ren, S. (2024). Risk assessment of heavy metals in agricultural soil based on the coupling model of Monte Carlo simulation–triangular fuzzy number. Environmental Geochemistry and Health, 46(2): 62. https://doi.org/10.1007/s10653-024-01866-y

Yan, H., Yao, X., Li, Y., & Xiong, Z. (2025). Capital market liberalization and corporate ESG rating divergence: a quasi-natural experiment based on the trading system of SSHC. Applied Economics, 57(60), 11107-11121. https://doi.org/10.1080/00036846.2025.2449849

Yousefi, H., Lak, E., Mohammadi, M.J. (2022). Carcinogenic risk assessment among children and adults due to exposure to toxic air pollutants. Environmental Science and Pollution Research, 29: 23015–23025. https://doi.org/10.1007/s11356-021-17300-0

Zahra, A., Hashmi, M.Z., Malik, R.N., Ahmed, Z. (2014). Enrichment and geo-accumulation of heavy metals and risk assessment of sediments of the Kurang Nallah—Feeding tributary of the Rawal Lake Reservoir, Pakistan. Science of the Total Environment, 470–471: 925–933. https://doi.org/10.1016/j.scitotenv.2013.10.017

Zhang, X., Li, D., Yan, H., & Ma, S. (2025). Does Air pollution affect the green innovation of industrial enterprises? Insights from Urban Sewage Control Policies in China. Global NEST Journal, 27(6), 1-14.

Zhanibekov, A., Issayeva, R., Golovatyi, S., Taspoltayeva, A., Aitimbetova, A., Nurtayeva, A., Kurganbekov, Z., Tulbasiyeva, A. (2022). Assessment of soil contamination by heavy metals: A case of Turkistan Region. Polish Journal of Environmental Studies, 31(2): 1985–1993. https://doi.org/10.15244/pjoes/142613

Zhou, L., Zhao, X., Meng, Y., Fei, Y., Teng, M., Song, F., Wu, F. (2022). Identification priority source of soil heavy metals pollution based on source-specific ecological and human health risk analysis in a typical smelting and mining region of South China. Ecotoxicology and Environmental Safety, 242: 113864. https://doi.org/10.1016/j.ecoenv.2022.113864

Zwolak, A., Sarzyńska, M., Szpyrka, E., Stawarczyk, K. (2019). Sources of soil pollution by heavy metals and their accumulation in vegetables: A review. Water, Air, and Soil Pollution, 230: 164. https://doi.org/10.1007/s11270-019-4221-y

Table S1. Sampling points and geographic coordinates in decimal degrees of 25 soil samples from the Annaba City region.

Points	Longitude(X)	Latitude(Y)
P-01	7.723333	36.918056
P-02	7.734722	36.918056
P-03	7.745833	36.918056
P-04	7.756667	36.918056
P-05	7.7652	36.918056
P-06	7.723333	36.909167
P-07	7.734722	36.909167
P-08	7.745833	36.909167
P-09	7.756667	36.909167
P-10	7.768056	36.909167
P-11	7.723333	36.9
P-12	7.734722	36.9
P-13	7.745833	36.9
P-14	7.756667	36.9
P-15	7.768056	36.9
P-16	7.723333	36.890556
P-17	7.734722	36.890556
P-18	7.745833	36.890556
P-19	7.756667	36.890556
P-20	7.7652	36.890556
P-21	7.723333	36.881944
P-22	7.734722	36.881944
P-23	7.745833	36.881944
P-24	7.756667	36.881944
P-25	7.7652	36.881944

Table S2. Positions and pH of 25 soil samples from the Annaba City region.

Positions	pH
P-01	7.5
P-02	7.7
P-03	7.8
P-04	7.7
P-05	7.7
P-06	7.8
P-07	7.8
P-08	7.7
P-09	7.6
P-10	7.7

P-11	7.7
P-12	7.7
P-13	7.7
P-14	7.6
P-15	7.6
P-16	7.5
P-17	7.4
P-18	7.2
P-19	7.3
P-20	7.9
P-21	7.5
P-22	7.7
P-23	7.6
P-24	7.6
P-25	7.9

Table S3. Concentrations of Cu, Cr and Cd in the soils from the Annaba City region ($mg.kg^{-1}$) compared to the French regulatory limits according to AFNOR U44-041 and the background value in the soil.

Position	Cd	Cu	Cr
P-01	0.12	36.82	32.05
P-02	0.30	30.56	72.10
P-03	0.14	45.35	23.25
P-04	0.28	35.23	80.57
P-05	0.15	50.54	35.24
P-06	0.18	37.45	48.23
P-07	0.37	41.28	15.24
P-08	0.46	36.95	34.89
P-09	0.36	41.66	49.68
P-10	2.57	37.52	62.54
P-11	0.43	41.54	31.56
P-12	0.30	39.94	78.25
P-13	0.28	99.68	108.90
P-14	6.08	87.56	54.58
P-15	1.18	85.86	42.56
P-16	0.36	68.65	69.63
P-17	0.14	45.87	56.28
P-18	1.71	52.24	45.92
P-19	10.15	106.35	121.24
P-20	1.30	109.68	55.43
P-21	0.54	87.56	85.38
P-22	0.39	136.85	47.39
P-23	0.62	152.17	58.36
P-24	14.01	105.64	69.45
P-25	1.11	123.19	70.56
Min	**0.12**	**30.56**	**15.24**
Max	**14.01**	**152.17**	**121.24**
Interval	0.12 – 14.01	30.56 – 152.17	15.24 – 121.24
Mean	1.74	69.45	57.97
Background values	0.097	22.6	61
Regulatory limit	2	100	150